Supplementary Materials for

A Mechano-diffusion Characterization Platform for Probing Strain-Programmable Nanoparticle Diffusion in Hydrogels

The PDF file includes:
Supplementary Notes
Fig. S1 to S9
Notes for Movies
References

Other Supplementary Materials for this manuscript include the following:
Movies S1 and S2

Supplementary Notes

AuNPs size distribution evaluation

We use MATLAB to analyze TEM images of AuNPs to quantify the size distribution of the core diameter of AuNPs. **Figure S1A** shows the TEM image of the first type of AuNPs. By analyzing the size distribution through a Gaussian fit (**Fig. S1C**), we identify the mean particle diameter as 6 nm. Similarly, **Figure S1B** and **S1D** show the TEM image and corresponding particle diameter distribution of the second type of AuNPs, respectively. We denote the mean value as the measured particle diameter for each type of AuNPs [1].

Diffusivity characterization

To extract the diffusivity, we use the numerical finite differential method (FDM) implemented in MATLAB to solve the diffusion governing equation in the cylindrical coordinate system. We first use MATLAB to obtain the grayscale values from the captured images of the diffusion profile, where the intensity of the grayscale value represents the concentration of the AuNPs. Thereafter, we fit the governing diffusion equation to these experimentally extracted grayscale values to determine the diffusivity. The governing diffusion equation in the Cartesian coordinate system is as follows

$$\frac{\partial c}{\partial t} = D\frac{\partial^2 c}{\partial x^2} \tag{S1}$$

where c is concentration, t is diffusion time, x is diffusion distance, and D is diffusivity. In the cylindrical coordinate system, **Eq. (S1)** can be further expressed as:

$$\frac{\partial c}{\partial t} = D\left(\frac{1}{r}\frac{\partial}{\partial r}\left(r\frac{\partial c}{\partial r}\right) + \frac{1}{r^2}\frac{\partial^2 c}{\partial \theta^2} + \frac{\partial^2 c}{\partial z^2}\right) \tag{S2}$$

where r is the diffusion distance along the radial direction, z is the axial distance, θ is the angular coordinate. Since the diffusion is symmetrical in the angular direction, namely $\partial c/\partial\theta = 0$, the **Eq. (S2)** can be further simplified as:

$$\frac{\partial c}{\partial t} = D\left(\frac{1}{r}\frac{\partial}{\partial r}\left(r\frac{\partial c}{\partial r}\right) + \frac{\partial^2 c}{\partial z^2}\right) = D\left(\frac{\partial^2 c}{\partial r^2} + \frac{1}{r}\frac{\partial c}{\partial r} + \frac{\partial^2 c}{\partial z^2}\right) \tag{S3}$$

In this study, the cylindrical sample occupies the domain where $-9 < r < 9$ and $0 < z < 6$ in millimeters as illustrated in **Fig. S2**. The concentration of AuNPs in the reservoir that occupies the domain where $-1.5 < r < 1.5$ and $3 < z < 6$ is set as a constant $c = c_0$; and the initial concentration in the other domain of the sample is set as $c = 0$. We further adopt the finite differential methods in MATLAB to numerically solve **Eq. (S3)**. By projecting the concentration profiles in the whole domain to the plane $z = 0$ and fitting the simulated concentration profile to the measured concentration profile, we can determine the measured diffusivity D as summarized in **Fig. S3 - S6**.

Relaxation time of the polymer network estimation

A PAAm sample, measuring 20 mm × 20 mm × 3 mm (length × width × thickness), is prepared for the experiments. As illustrated in **Fig. S7A**, the sample is instantaneously stretched to a stretch ratio of $\lambda = 4.0$ over a stretching time 8 seconds, as shown in **Fig. S7B**, and then held for sufficient duration. The nominal stress versus time curve is shown in **Fig. S7C**. We use the Maxwell model, expressed in **Eq. S4**, to identify the relaxation time as 19.4 seconds [2],

$$\frac{S(t) - S_{min}}{S_{max} - S_{min}} = e^{-\left(\frac{t}{t_m}\right)} \qquad (S4)$$

where S_{max} and S_{min} are the maximum and minimum nominal stress, the t is time, and t_m is the relaxation time of the material. The decrease in nominal stress can be attributed to the polymer network relaxation and the migration of the solvent [3]. In our mechano-diffusion experiments, the loading/unloading period is 2 seconds, significantly shorter than the relaxation time of the polymer network. Therefore, the rapid loading rate is sufficient to influence the hopping diffusion process in the hydrogel.

Tough glass-hydrogel bonding techniques

The hydrogel is bonded to the upper and lower glass slides using saline chemistry, following the protocol reported in the literature [4] (**Fig. S8**). After treatment with the TMSPMA solution, the PAAm hydrogel forms a robust bond with the glass slides [4]. The assembly structure of the hydrogel-glass-AuNPs solution system is depicted in **Fig. S9**. As illustrated in **Fig. S9A**, the upper glass slide has a hole for filling with the AuNPs solution, while the lower glass slide remains intact. During the observation of diffusion profiles in the hydrogel sample, the acrylic parts are disassembled and removed, as shown in **Fig. S9B**.

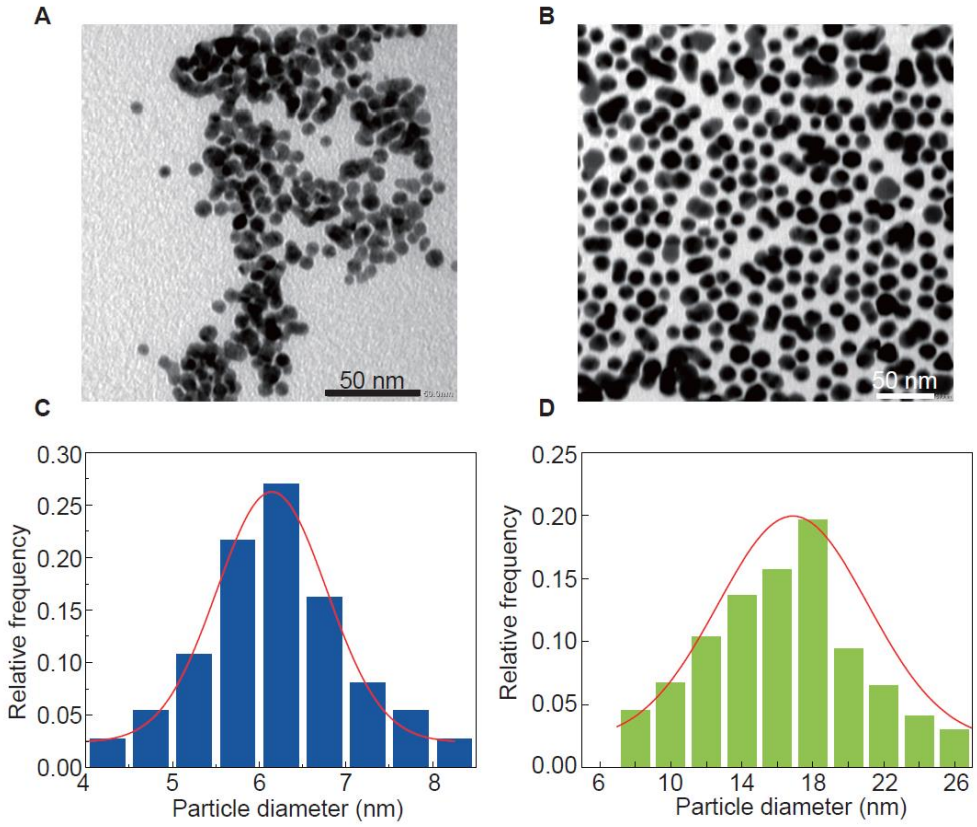


Fig. S1. TEM characterization of AuNP diameter distribution. A) The TEM image of the 6 nm diameter AuNPs. **B)** The TEM image of the 18 nm diameter AuNPs. **C)** The histogram in the plot of relative frequency as a function of particle diameter, identifying the particle diameter of the first set of AuNPs as 6 nm. The red curve is the corresponding Gaussian fit. **D)** The histogram in the plot of relative frequency as a function of particle diameter, identifying the particle diameter of the first set of AuNPs as 18 nm. The red curve is the corresponding Gaussian fit. The scale bars in **A)** and **B)** are 50 nm.

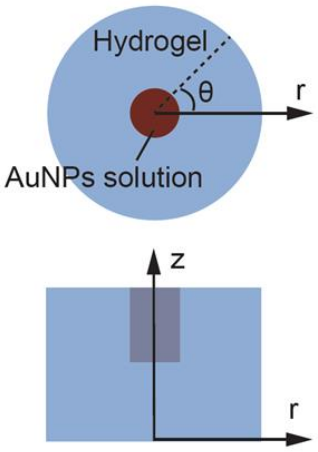


Fig. S2. Cylindrical coordinate system for diffusivity evaluation. The radial axis *r* and the axial axis *z* have their origins at the bottom surface of the sample, and the angular axis θ is defined in the anti-clockwise direction.

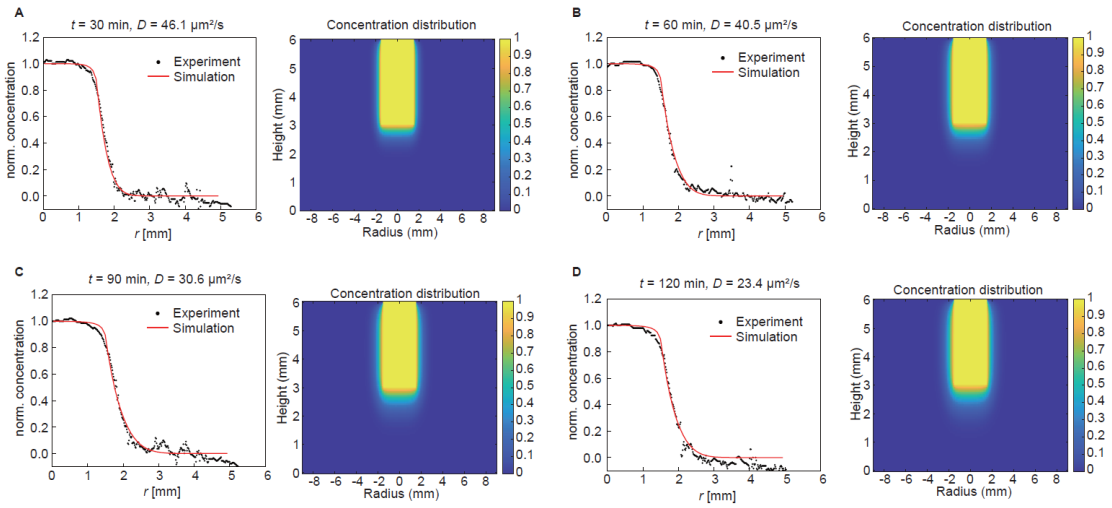


Fig. S3. Extraction of the diffusivity of 6 nm diameter AuNPs in hydrogels under dynamic tension. Comparison of the diffusion profiles between measured experimental results and fitted simulation curves, identifying the particle diffusivity as **A)** 46.1 $\mu m^2/s$ at the time of 30 min, **B)** 40.3 $\mu m^2/s$ at the time of 60 min, **C)** 30.6 $\mu m^2/s$ at the time of 90 min, and **D)** 23.4 $\mu m^2/s$ at the time of 120 min.

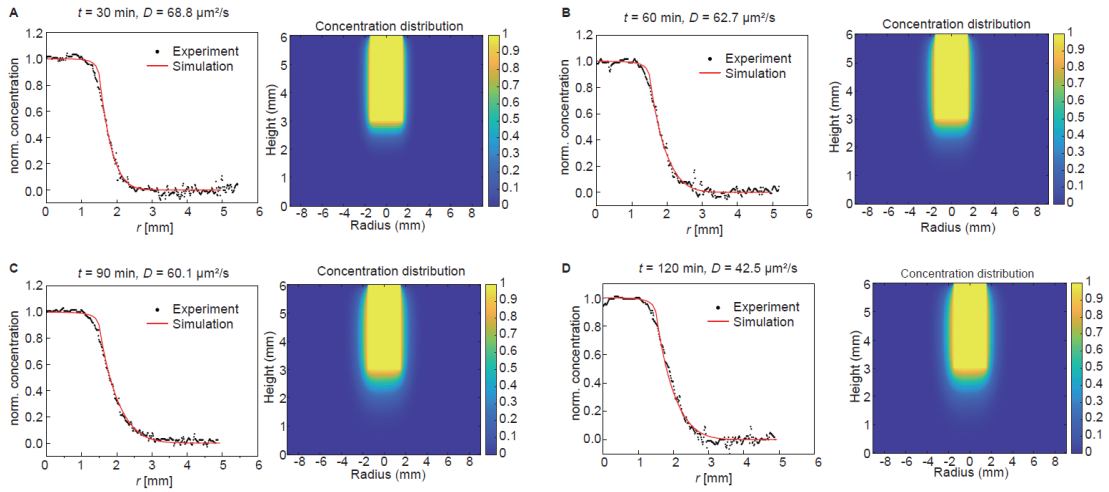


Fig. S4. Extraction of the diffusivity of 6 nm diameter AuNPs in hydrogels under static load. Comparison of the diffusion profiles between measured experimental results and fitted simulation curves, identifying the particle diffusivity as **A)** 68.8 $\mu m^2/s$ at the time of 30 min, **B)** 62.7 $\mu m^2/s$ at the time of 60 min, **C)** 60.1 $\mu m^2/s$ at the time of 90 min, and **D)** 42.5 $\mu m^2/s$ at the time of 120 min.

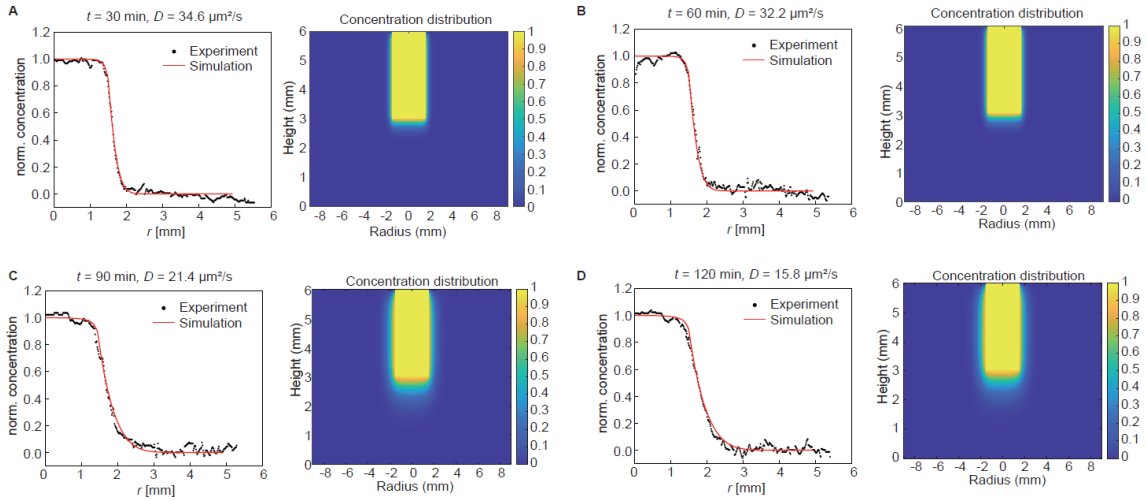


Fig. S5. Extraction of the diffusivity of 18 nm diameter AuNPs in hydrogels under dynamic load. Comparison of the diffusion profiles between measured experimental results and fitted simulation curves, identifying the particle diffusivity as **A)** 34.6 $\mu m^2/s$ at the time of 30 min, **B)** 32.2 $\mu m^2/s$ at the time of 60 min, **C)** 21.4 $\mu m^2/s$ at the time of 90 min, and **D)** 15.8 $\mu m^2/s$ at the time of 120 min.

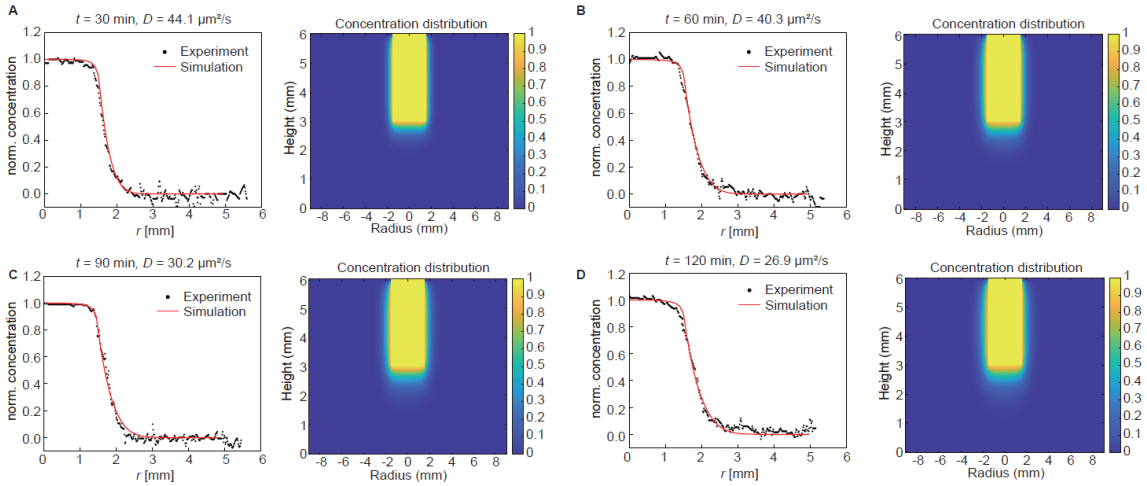


Fig. S6. Extraction of the diffusivity of 18 nm diameter AuNPs in hydrogels under static load. Comparison of the diffusion profiles between measured experimental results and fitted simulation curves, identifying the particle diffusivity as **A)** 44.1 $\mu m^2/s$ at the time of 30 min, **B)** 40.3 $\mu m^2/s$ at the time of 60 min, **C)** 30.2 $\mu m^2/s$ at the time of 90 min, and **D)** 26.9 $\mu m^2/s$ at the time of 120 min.

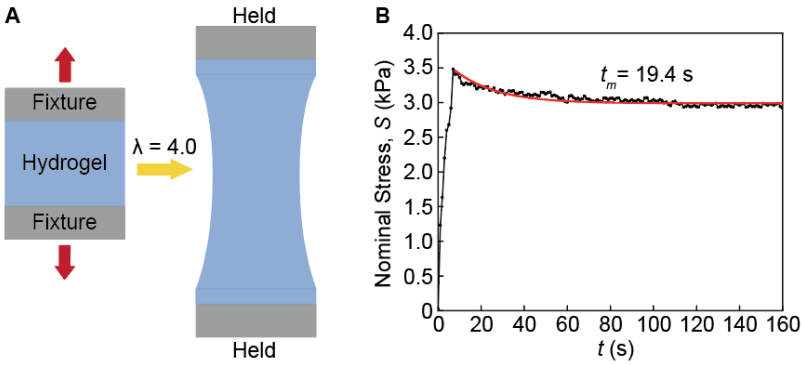


Fig. S7. **Stress relaxation experiment of the PAAm hydrogel. A)** The schematics of the experimental setup, where the hydrogel is stretched to a ratio of 4.0 and held at this fixed stretch ratio. **B)** The nominal stress versus time curve from the experiment and the corresponding fitting curve.

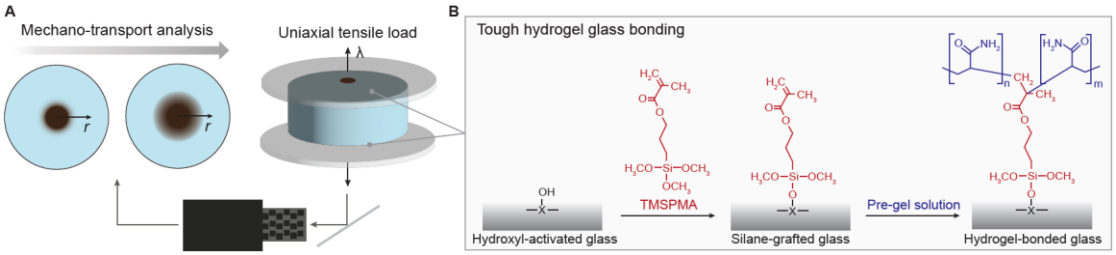


Fig. S8. AuNPs transport experiment setup and glass-hydrogel bonding chemistry. A) The imaging system of the mechano-transport experiment. **B)** the hydrogel-glass bonding chemistry.

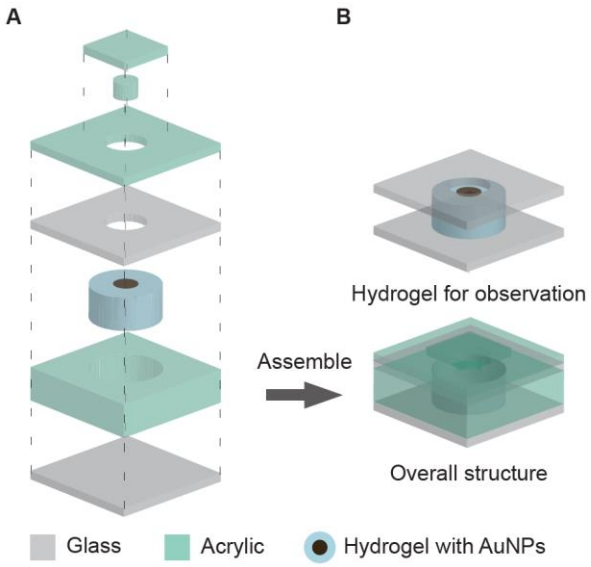


Fig. S9. Device fabrication for the uniaxial mechano-transport characterization platform. Schematic illustrations of **A)**, assembling a cylindrical acrylic rod, an acrylic plate, a cover glass, a cylindrical hydrogel, an acrylic mold, and a glass slide into **B)**, the uniaxial mechano-transport characterization platform.

Notes for Movies

Movie S1. The silicon rubber under cyclic tensile load applied by MDCP and corresponding stress-time curve.

This video shows that the silicon rubber is under the cyclic tensile load applied by MDCP and corresponding stress-time curve of the sample.

Movie S2. The silicon rubber under cyclic torsion load applied by MDCP and corresponding torque-time curve.

This video shows that the silicon rubber is under the cyclic torsion load applied by MDCP and corresponding torque-time curve of the sample.

References

1 Gorbachev, E. *et al.* Tuning the particle size, natural ferromagnetic resonance frequency and magnetic properties of ε-Fe 2 O 3 nanoparticles prepared by a rapid sol–gel method. *Journal of Materials Chemistry C* **9**, 6173-6179 (2021).

2 Sánchez, E., Nájera, A. & Sotomayor, O. Numerical study of the viscoelastic mechanical response of polystyrene in the process of thermoforming through the generalized Maxwell model. *Materials Today: Proceedings* **49**, 107-114 (2022).

3 Hu, Y., Zhao, X., Vlassak, J. J. & Suo, Z. Using indentation to characterize the poroelasticity of gels. *Applied Physics Letters* **96** (2010).

4 Yuk, H., Zhang, T., Lin, S., Parada, G. A. & Zhao, X. Tough bonding of hydrogels to diverse non-porous surfaces. *Nature materials* **15**, 190-196 (2016).